



In-Silico Assessments of Fruticulin-A and Demethylfruticulin-A Isolated from *Salvia* Species Against Important Anticancer Targets

Hossein Hadavand Mirzaei ^{*}, Seyed Mohammad Hosseini

Department of Molecular Physiology, Agricultural Biotechnology Research Institute of Iran, Agricultural Research, Education and Extension Organization (AREEO), Karaj, Iran.

Abstract

Background and objectives: Bioactive compounds derived from plants have been used to treat various ailments with minimal adverse effects. The in-silico methods are developed to predict the behavior of drug candidates before performing the in-vitro and in-vivo experiments. In the current study, a computational investigation was conducted to understand the probable mechanisms of two benzoquinone diterpenoids namely fruticulin-A and demethylfruticulin-A isolated from several *salvia* species by molecular docking and dynamic simulation approaches. **Methods:** The above mentioned compounds with proven anticancer activity were docked against five selected target proteins that regulate cell proliferation and apoptosis including cyclin-dependent protein kinase 2 (CDK-2), CDK-6, DNA topoisomerases I (topo I), topo II and B-cell lymphoma-2 (Bcl-2) using autodock 4.2. Besides, molecular dynamics simulations were applied to evaluate the stability of the best-docked complexes. **Results:** Both compounds demonstrated remarkable binding affinity to CDK-2 than the known CDK-2 inhibitor. The trajectory analysis for 50 nanosecond (ns) revealed acceptable RMSD, RMSF and Rg values during the entire molecular dynamic simulation which confirmed the stability of complexes. **Conclusion:** The results of our study displayed that fruticulin-A and demethylfruticulin-A can be developed as excellent natural product derived CDK-2 inhibitors, and further biological experiments should be performed to confirm their use as an efficient option for treating cancer disease.

Keywords: anticancer; demethylfruticulin-A; fruticulin-A; molecular docking; molecular dynamics

Citation: Hadavand Mirzaei H, Hosseini SM. In-silico assessments of fruticulin-A and demethylfruticulin-A isolated from *Salvia* species against important anticancer targets. Res J Pharmacogn. 2023; 10(3): 31–41.

Introduction

Cancer is the second leading cause of morbidity and mortality after cardiovascular disease all over the world. At the moment, several certain chemotherapeutic agents are available on the market for the treatment of different types of cancer such as taxol, anthracycline, vincristine, herceptin and ixabepilone. However, the high cost, side effects and drug resistance of anticancer drugs are major reasons for the identification of potent and novel anticancer agents [1,2]. Based on reports and evidence, the discovery of a new drug is a time-consuming and

complex procedure. Research projects on drug discovery have shown that the biggest challenges in drug development are related to the initial phases where unexpected toxicity and adverse drug reactions cause more than 40% of the drug candidates to fail. In-silico methodology with minimum cost can help us to decrease failures in the drug discovery process. Furthermore, the usage of this technique reduces both the time needed to bring a drug to the market and also killing animals for predicting toxicological parameters [3].

* Corresponding author: h_hadavand@abrii.ac.ir

In the recent decades, secondary metabolites derived from natural products have played a vital role in the development of the anticancer drugs, whereas around 60% of anticancer-approved drugs were found from these metabolites [4].

The genus *Salvia* (Lamiaceae) with around 900 species is well-known as a rich source of triterpene and diterpene compounds with several biological properties. The benzoquinone diterpenoids, fruticuliculin-A and demethylfruticuliculin-A were isolated as major compounds of *S. lachnostachys*, *S. fruticulosa*, *S. arizonica* and *S. corrugata* with a broad spectrum of pharmacological activities such as cytotoxicity, antibacterial, anti-inflammatory and antihyperalgesic properties [5-9]. Recently, both compounds have shown significant cytotoxic activity through inhibition of HDACs (histone deacetylases family) and induction of apoptosis in cancer cells [10-12].

The above information led us to design a computational study for the prediction of the druggability and mode of action of these compounds. Therefore, the docking studies were performed to assess the possible binding and molecular interactions of these compounds with five selected target proteins that regulate cell proliferation and apoptosis including cyclin-dependent protein kinase 2 (CDK-2), CDK-6, DNA topoisomerases I (topo I), topo II and B-cell lymphoma-2 (Bcl-2) using autodock 4.2 (ADT). Then, using GROMACS 5.1.4 software package, molecular dynamic (MD) simulation studies were applied for validation of the docked complexes of ligand-protein.

Material and Methods

Ethical considerations

Relevant research ethics have been fully considered during this study.

Evaluation of molecular physicochemical and pharmacokinetic properties

Assessment of the physicochemical profile of any compounds such as druglike properties and toxicity are the initial parameters of drug development. In the present study, ADMET (absorption, distribution, metabolism, excretion, and toxicity) was calculated using the open-source tool swiss ADME (<http://www.swissadme.ch/index.php>).

Furthermore, the pharmacokinetic values were obtained using the online platform pkCSM (<http://biosig.unimelb.edu.au/pkcsm/prediction>) [13].

Preparation of ligands

The three-dimensional structures (3D) of fruticuliculin-A and demethylfruticuliculin-A (Figure 1) with proven anticancer activity were retrieved from PubChem data bank in SDF format (<http://pubchem.ncbi.nlm.nih.gov>). In the next step, according to our previously described protocol, these structures were optimized using the Gaussian 09 program [14]. The outputs of G09 were converted to pdb format by openbuble software and then used for molecular docking studies. Finally, the gasteiger partial atomic charges of optimized molecules were added by ADT and saved in pdbqt format.

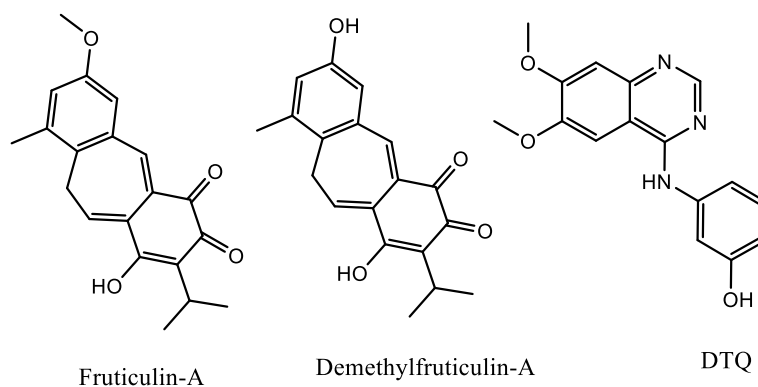


Figure 1. Structures of fruticuliculin-A, demethylfruticuliculin-A and 4-[3-Hydroxyanilino]-6,7-Dimethoxyquinazoline (DTQ)

Preparation of protein target structure

The X-ray crystallographic structure of five selected protein receptors including CDK-2 (PDB ID: 1DI8), CDK-6 (PDB ID: 1XO2), topo I (PDB ID: 1T8I), topo II (PDB ID: 1ZXM) and Bcl-2 (PDB ID: 2O2F) were downloaded from RCSB protein data bank. Missing amino acid residues of each pdb file of protein targets were checked by notepad⁺⁺ software and then the missing residues were modelled and added in the incomplete structures using Modeller 9.17 program [15]. The modeled crystal structure was validated by Ramachandran plot using Procheck server (<https://saves.mbi.ucla.edu/>). Then, co-crystallized ligands and water molecules were removed from crystal structures. In the next step, all polar hydrogen atoms were added and Kollman charges were assigned to the proteins and saved in pdbqt format by ADT.

Molecular docking studies

The performance of each docking system was validated by self-docking of the native ligand into the active site of its respective target. Docking studies of fruticulín-A and demethylfruticulín-A were performed against mentioned protein targets using autodock 4.2 [16]. The grid maps were determined based on the coordinates of native ligands in X-ray crystal structures. The details of grid box properties are indicated in Table 1. The compounds were docked to the active site of the selected receptor using the Lamarckian genetic algorithm with the maximum number of evaluations set to 2.5×10^6 , the number of GA runs was 100, the maximum number of generations was set as 27,000, and all of the other options were set as default. For interpretation of docking results, the conformations with the lowest free energy of binding (ΔG) and the

lowest inhibition constant (K_i) from the largest population cluster were selected. The docking outputs were subjected to LigPlot⁺ software for visualization of the interaction between ligands and receptors.

Molecular dynamics simulations

The molecular dynamics (MD) simulation of the docked ligand-CDK2 complexes were undergone for 50 ns using GROMACS 5.1.4 software package with CHARMM36 force field for protein docked complexes.

To obtain ligands compatible with the CHARMM force field, topology files of ligands were generated using the CGenFF web server. The complexes were solvated with a TIP3P explicit water model (SPC216) in a 3-D cube box and the spacing between the solute and the box edge was adjusted to 1.0 nm. Then, the systems of individual complexes were consequently neutralized by adding Cl⁻ counter ions. The steepest descent algorithm was used for energy minimization of complexes during a 100 ps simulation. In the next step, the reference temperature and pressure were set to 300 K and 1 bar respectively and the complexes were equilibrated in NVT (number of particles, volume and temperature) and NPT ensemble (number of particles, pressure and temperature) for 100 ps run time. The V-rescale thermostat and the Berendsen method were applied to keep the temperature and pressure constant, respectively. The long-ranged electrostatic contributions were calculated with particle mesh ewald (PME) method and the geometry of all of the bond lengths was constrained using the LINCS algorithm. Then, the equilibrated complexes were subjected to production MD run for 50 ns.

Table 1. The details of grid box properties

Macromolecular Target	Co-crystal ligand	PDB ID	Grid box dimensions		
			No. of grid points (npts)	Center (X,Y,Z coordinates)	Grid point spacing (Å)
CDK-2	4-[3-Hydroxyanilino]-6,7-Dimethoxyquinazoline (DTQ)	1DI8	60×60×60	-7.623, 49.881, 11.367	0.375
CDK-6	3,7,3',4'-Tetrahydroxyflavone (FSE)	1XO2	60×60×60	-3.142, 37.712, 139.104	0.375
Topoisomerase I	4-Ethyl-4-Hydroxy-1,12-Dihydro-4h-2-Oxa-6,12a-Diaza-Dibenzo[B,H]Fluorene-3,13-Dione (EHD)	1T8I	60×60×60	20.935, -1.307, 27.99	0.375
Topoisomerase II	Phosphoaminophosphonic Acid-Adenylate Ester (ANP)	1ZXM	60×60×60	31.89, -0.566, 38.576	0.375
Bcl-2	4-(4-Benzyl-4-Methoxypiperidin-1-Yl)-N-[(4-[[1,1-Dimethyl-2-(Phenylthio)Ethyl]Amino]-3-Nitrophenyl)Sulfonyl]Benzamide (LI0)	2O2F	65×65×65	-0.024, 3.142, 0.361	0.375

Finally, we calculated the Root Mean Square Deviation (RMSD) nm for the protein backbone atoms of the protein throughout the MD simulations regarding the initial frame. Also, we monitored the movements of residue atoms by calculating of the root means square fluctuation (RMSF) for the backbone atoms of proteins.

Results and Discussion

Exact estimations during initial ADMET screening can reduce the failures in pre-clinical and clinical phases. Based on Lipinski's rule of five, the substances with more than 5 H-bond donors, 10 H-bond acceptors, a molecular weight greater than 500 Da and the obtained LogP (CLogP) greater than 5 (or MlogP>4.15) are classified as compounds with poor absorption or permeation. In addition, a compound can be considered for good bioavailability if it follows these criteria: rotatable bonds \leq 10 and total polar surface area (TPSA) of \leq 140 Å. The prediction of the physicochemical characteristics of both compounds is illustrated in Table 2. The results indicated that both compounds were found to obey Lipinski's limit range. The oral

bioavailability of both compounds was predicted, based on a calculation of the lipophilicity, insolubility, size, insaturation, polarity, and flexibility of both compounds using the online platform swiss ADME [17]. The oral bioavailability graph for fruticulín-A and demethylfruticulín-A is shown in Figure 2A. The pharmacokinetics parameters of both compounds are presented in Table 3. As mentioned in Table 3, both showed middle absorption to the central nervous system (CNS) because the blood-brain barrier (BBB) penetration was between 2.0 and 0.1. Moreover, fruticulín-A and demethylfruticulín-A displayed high gastrointestinal absorption (GI) with more than 90% absorption. The results suggest that these compounds can be optimized as oral drugs.

The BOILED-EGG plot as one of the outcomes from the swiss ADME database shows the ability of compounds for the BBB penetration and high gastrointestinal absorption (HIA) [18]. According to Figure 2B, our compounds were placed in a yellow circle and kept a distance from the center of the circle.

Table 2. Evaluation of physicochemical parameters and lipophilicity properties of fruticulín-A and demethylfruticulín-A

Property	Parameters	Fruticulín-A	Demethylfruticulín-A
Physicochemical Properties	MW ^a (g/mol)	324.37	310.34
	HBA ^b	4	4
	HBD ^c	1	2
	TPSA ^d	63.60	74.60
	Fraction Csp3	0.30	0.26
	Rotatable bonds	2	1
	No. violationse ^e	0	0
Lipophilicity	ILOGP	2.78	2.13
	XLOGP3	3.17	2.84
	MLOGP	1.85	1.62
	Consensus	3.06	2.65

^a Molecular weight; ^b H-bond acceptor; ^c H-bond donor; ^d topological polar surface area and; ^e number of Lipinski violations

Table 3. Computed pharmacokinetics parameters of fruticulín-A and demethylfruticulín-A

Property	Parameters	Fruticulín-A	Demethylfruticulín-A
Absorption	Water solubility (log mol/L)	-4.319	-4.066
	GI ^a	96.839	95.61
	Log Kp (skin permeation) cm/s	-3.666	-3.757
Distribution	BBB ^b	0.472	0.191
	CNS permeation (Log PS)	-1.176	-1.822
	VD ^c (human)	0.213	0.113
Metabolism CYP2D6	CYP1A2 inhibitor	No	No
	CYP2C9 inhibitor	No	No
	CYP2C19 inhibitor	Yes	No
	CYP3A4 inhibitor	Yes	No
	CYP2D6 inhibitor	No	No
Excretion	Total Clearance (log mL/min/kg)	0.135	0.082
	Renal OCT2 substrate	Yes	No

^a gastrointestinal; ^b blood-brain barrier; ^c volume of distribution

These positions in the plot indicated that our compounds had poor BBB penetration and a well GI absorption. Results also revealed that neither of the compounds acted as inhibitors of P-glycoprotein (Pgb), which plays a critical role in drug resistance in cancer cells by drugs efflux. The high negative values of Log Kp demonstrated low skin permeation for the tested compounds. Based on our results, demethylfruticulin-A was found to be a non-inhibitor of cytochrome isoform which indicates this compound will be rapidly metabolized. On the other hand, fruticulin-A showed inhibiting activity against two cytochrome isoforms including CYP2C19 and CYP3A4. The toxicity of both compounds were predicted using the AMES test and the compounds did not show any acute toxicity (Table 4). Nonetheless, the main drawback of demethylfruticulin-A was its hepatotoxicity which this must be a concern in clinical studies.

Assessment of protein structures showed that all of the target proteins except Bcl-2 had missing residue. Therefore, the structure of proteins was repaired by modeller software. Then, the validation of structures was evaluated by the Ramachandran plot [19]. Ramachandran plots are presented in Figure 3. The ramachandran plot for these structures showed that more than 90% of residues were in the favorite and allowed regions of the plot (red and yellow zone) while only 0.2-

0.4 % of residues were in the disallowed zone (white zone) which indicated a good quality for protein structures.

We evaluated the performance and validation of the docking protocol before proceeding with molecular docking studies through a self-docking of the native ligands into their active sites. In all experiments, the RMSD was found to be $< 2 \text{ \AA}$ (Figure 4). According to acceptable RMSD of self-docking ($< 2 \text{ \AA}$), the obtained results indicated that the docking protocols were reliable. In the present study, docking was performed using autodock 4.2; two ligands namely fruticulin-A and demethylfruticulin-A were docked into the catalytic site of five different target proteins, including CDK-2, CDK-6, Topo I, Topo II and Bcl-2.

Table 4. Assessment of toxicity profile of fruticulin-A and demethylfruticulin-A

Parameters	Fruticulin-A	Demethylfruticulin-A
Ames Toxicity	No	No
Max. Tolerated Dose (human) (log mg/kg/day)	0.158	0.096
hERG I Inhibitor	No	No
hERG II Inhibitor	No	No
Oral Toxicity (LD50) (mg/kg)	2.174	2.131
Hepatotoxicity	No	Yes
Skin Sensitization	No	No
Fathead Minnow LC ₅₀ .Log ₁₀ (mmol/L)	-0.453	-0.061
<i>Tetrahymena pyriformis</i> IGC ₅₀ - Log ₁₀ (mol/L)	1.013	0.639

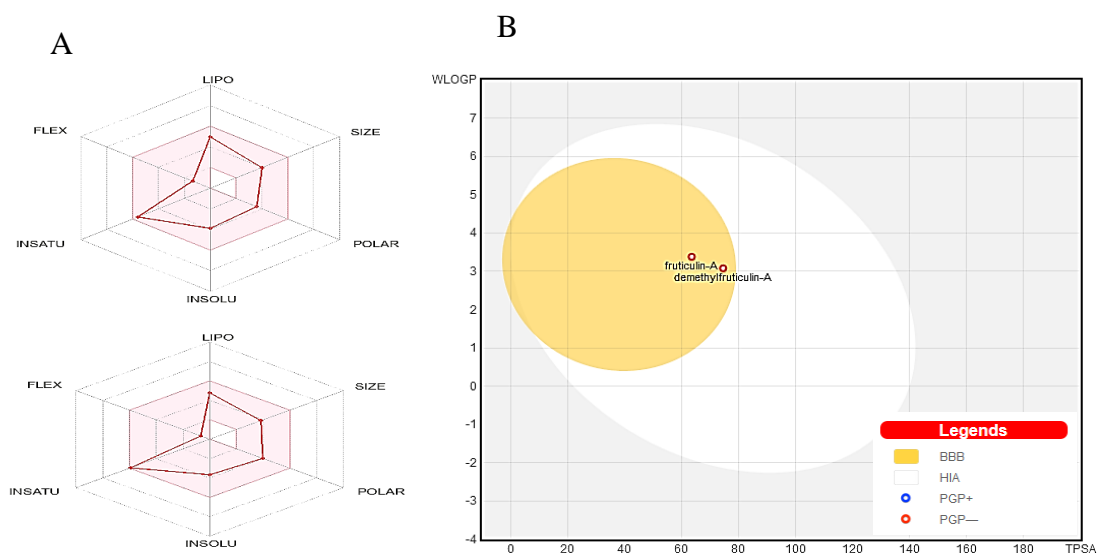


Figure 2. (A) Bioavailability radar chart fruticulin-A (up) and demethylfruticulin-A (down). The pink region represents the physicochemical space for oral bioavailability, and the red line represents the oral bioavailability properties; (B) predicted BOILED-Egg plot from swiss ADME for both compounds

The binding energies of both compounds and the native ligands are enumerated in Table 5. Regarding the obtained results, fruticulin-A and demethylfruticulin-A showed an outstanding binding affinity to CDK-2 with ΔG of - 8.17 and -8.39 kcal/mol and K_i of 820 and 629 nM even more than that of native ligand with ΔG of - 7.79 kcal/mol and K_i of 1270 nM. The docking results for reference compound DTQ with CDK-2 showed the formation of one hydrogen bond with Leu 83 of length 2.92 Å and residues involved in hydrophobic interactions, including Val 64, Phe 80, Ala 44, Lys 33, Val 18, Asp 86, Gln 131 Leu 34, Ile134, Ile10, His 84, Gln 85, Ala 31, Glu 81 and Phe 82 (Figure 5A). Fruticulin-A formed a

hydrogen bond with a distance of 2.91 Å apart from the Leu 83 basic amino acid residue of the CDK-2 active site. It also established the hydrophobic interactions via residues Asp 86, Gln 85, Phe 82, Phe 80, Ala 31, Val 18, Leu 32, Lys 33, Asp 145, Ala 144, Leu 134 and Ile 10 (figure 5B). In the docking pose, demethylfruticulin-A formed three H-bonds with Gln 131, Asp 145 and Lys 33 at distances of 2.74, 2.82 and 2.68 Å, respectively. The residues Ala31, Glu 81, Val 64, Leu 34, Ala 44, Phe 80, Val 18, Asn 132, Glu 12, and Gly 13 showed important hydrophobic interactions with this compound (Figure 5C).

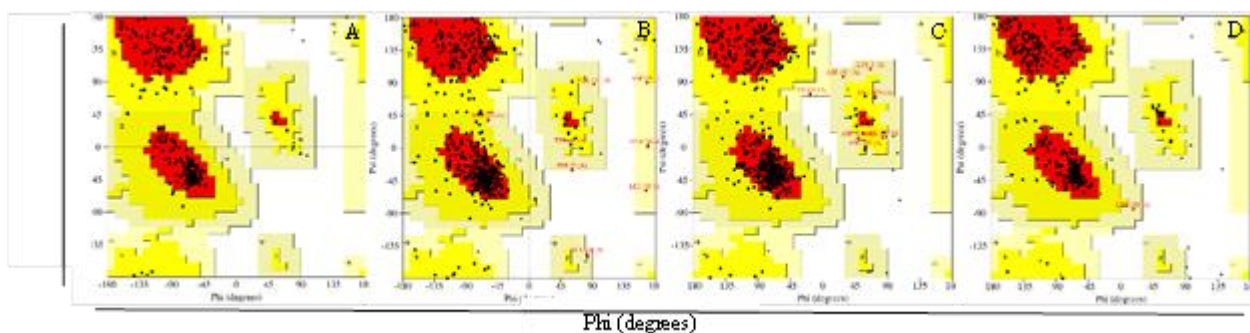


Figure 3. The ramachandran plot of the protein structures: (A) CDK-2, (B) CDK-6, (C) Topo I and (D) Topo II

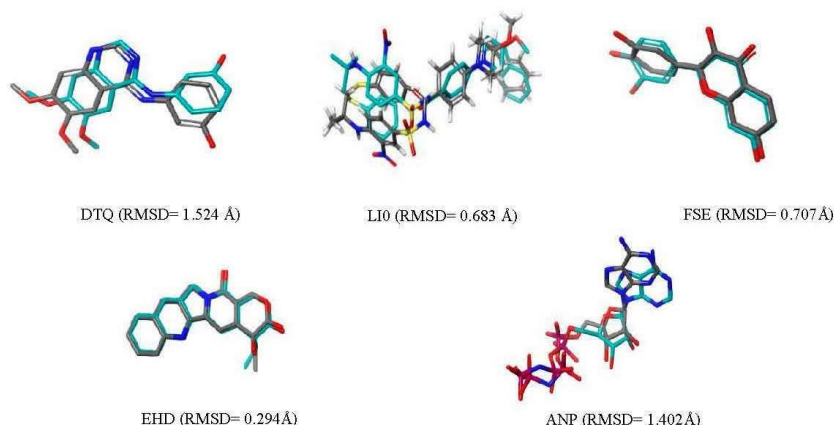


Figure 4. Validation of molecular docking results; the RMSDs were computed relative to the position of original co-crystal (cyan) and docked poses (gray) of the co-crystal ligands

Table 5. Binding free energies (BE) in kcal/mol and inhibition constant (K_i) in nM of fruticulin-A and demethylfruticulin-A docked against selected molecular targets

Ligands	Macromolecules Target									
	CDK-2		CDK-6		Topoisomerase I		Topoisomerase II		Bcl-2	
	BE	K_i	BE	K_i	BE	K_i	BE	K_i	BE	K_i
Fruticulin A	-8.17	820	-9.90	20.78	-8.99	225800	-8.89	281120	-7.23	4660
Demethylfruticulin A	-8.39	629	-9.74	43.36	-9.17	165180	-8.67	228440	-7.07	4860
Co-crystal ligands	-7.79	1270	-10.06	33.88	-10.81	11590	-10.05	2120	-9.83	8.78

The docked complexes of DTQ, fruticulin-A and demethylfruticulin-A with CDK-2 receptor were further studied using the MD simulations to monitor the conformational variation in an aqueous system for a simulation time of 50 ns. To visualize the dynamic behavior of CDK-2 with ligands, the snapshots from 0 to 50 ns of the docked complexes during MD simulations are indicated in Figure 6. The RMSDs of backbone atoms in CDK-2 were calculated through MD simulations to examine the stability of the system. As can be seen in Figure 7, initially, the large fluctuations in RMSD values were observed in the docked complexes up to 10 ns and then remained virtually constant throughout the

simulation averaging at 0.266 ± 0.026 nm, 0.277 ± 0.021 nm, 0.273 ± 0.024 nm, for CDK-2_DTQ, CDK-2_fruticulin-A and CDK-2_demethylfruticulin-A, respectively. Thus, the calculated RMSDs revealed that the CDK-2 protein was quite stable during the entire simulations. The root means square fluctuation (RMSF) estimates the deviation of the residues in the protein structure. The analysis of RMSFs in the CDK-2 protein backbone were found stable entire course simulation for all the complexes with values of 0.04 to 0.64 Å (Figure 8). The radius of gyration (Rg) can be defined as the root mean square distance from each atom of the macromolecules to its center of mass.

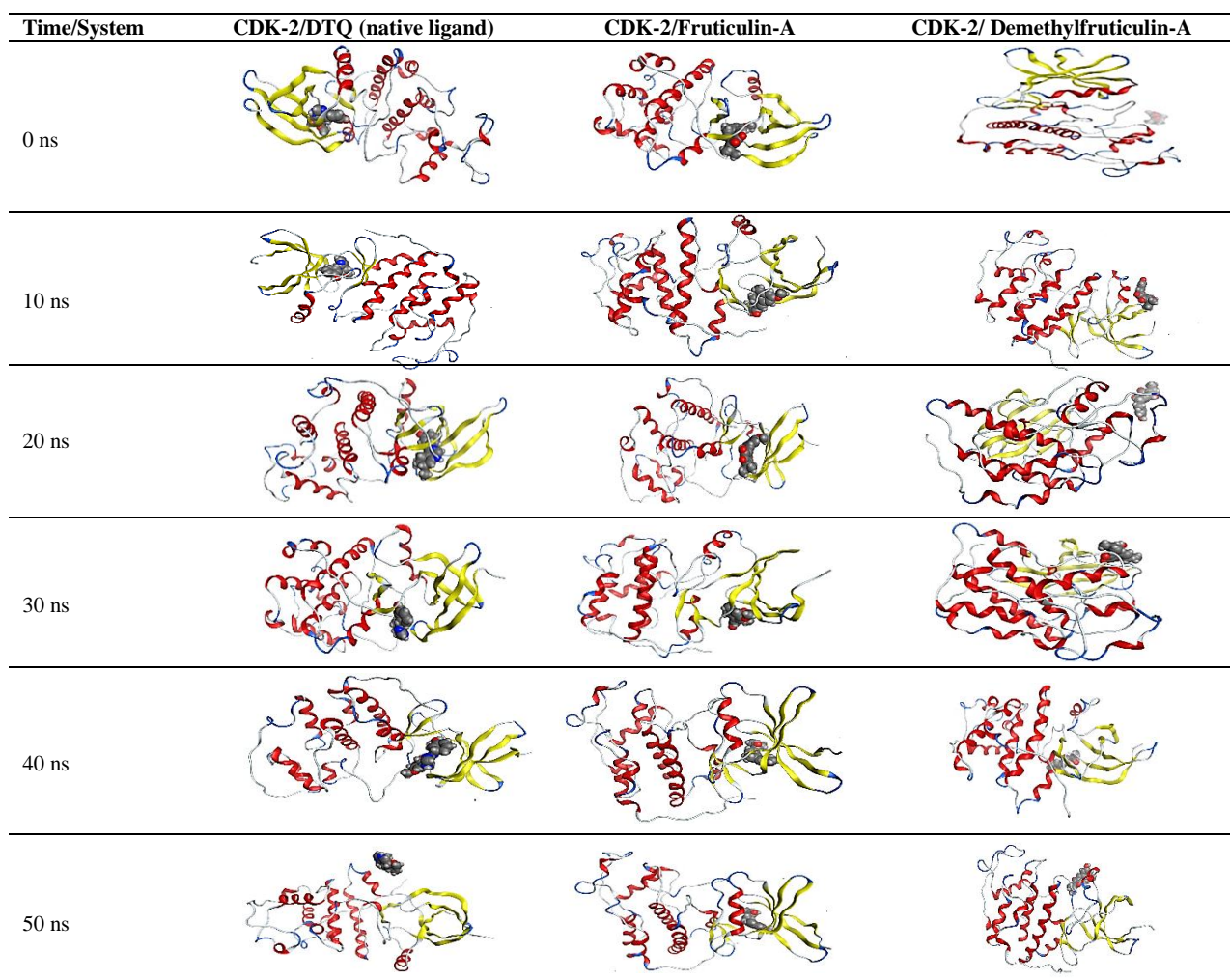


Figure 6. The snapshots of trajectories of the docked complexes from 0 to 50 ns MD simulation

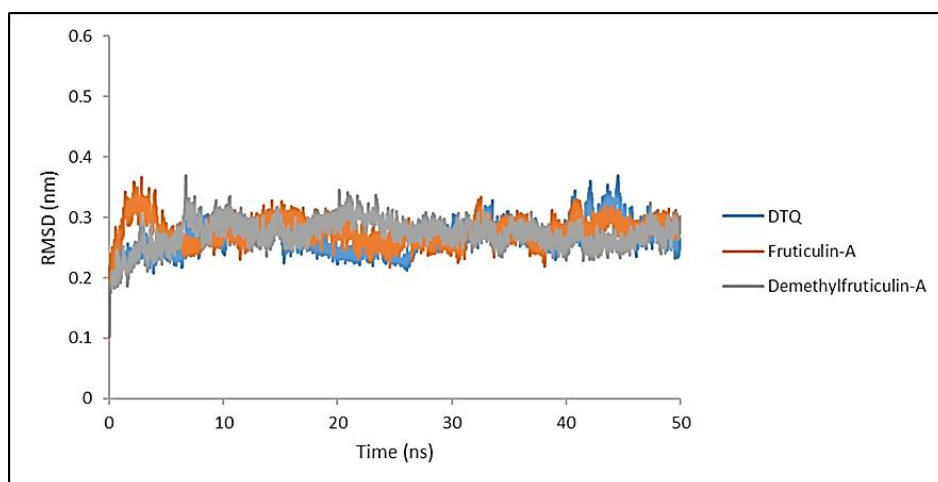


Figure 7. Root-mean-square deviation (RMSD) of backbone atoms in CDK2

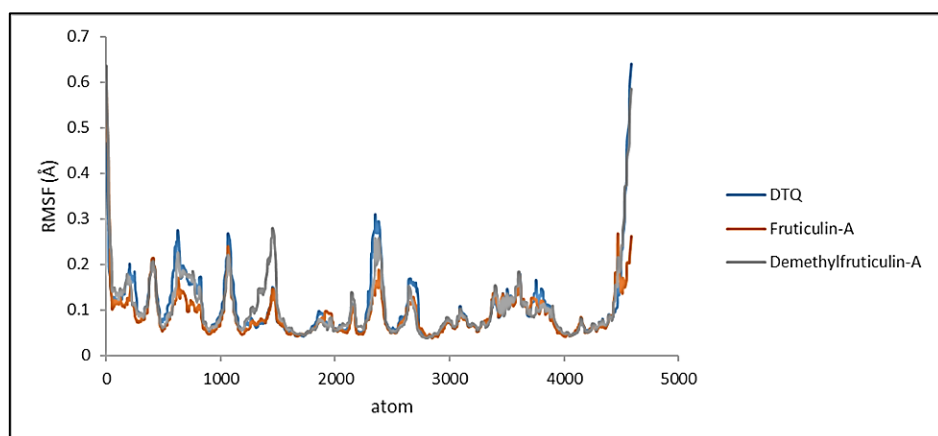


Figure 8. Plot of root-mean-square fluctuation of backbone atoms in CDK2 complexes

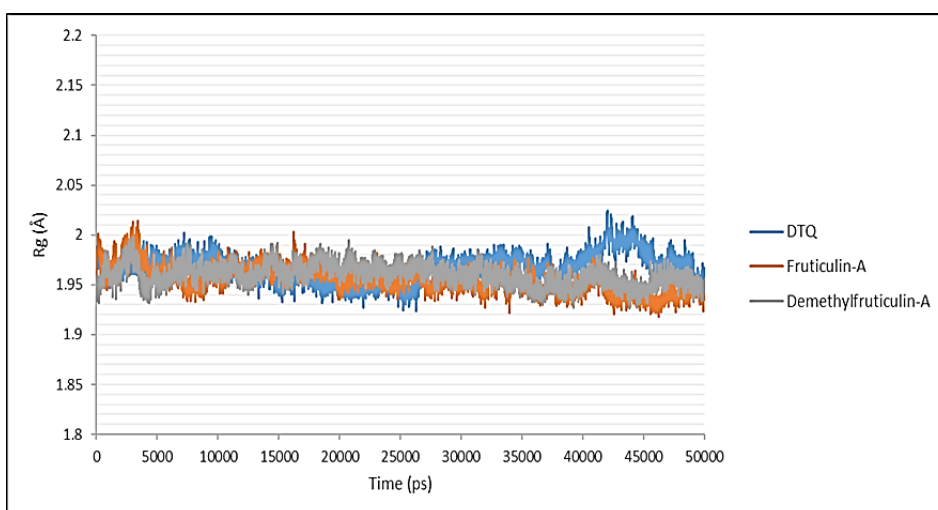


Figure 9. Variation in the radius of gyration (Rg)

The Rg values for protein-ligand complexes CDK-2_DTQ, CDK-2_fruticul-A and CDK-2_demethylfruticul-A show stable fluctuations between 1.924 to 2.024 Å, 1.918.1 to 2.014 Å, and 1.926 to 1.998 Å, respectively (Figure 9).

Conclusion

We applied a reverse docking strategy for the prediction of the mechanism of fruticul-A and demethylfruticul-A against important anticancer drug targets. Molecular docking results exhibited their binding potential with the targets through hydrogen bonds and hydrophobic interactions. Both compounds showed better binding affinity to CDK-2 than the known CDK-2 inhibitor. The best-docked complexes of ligand-protein showed an excellent range of RMSD, RMSF and Rg values during the entire of molecular dynamic simulation which confirmed the stability of complexes. Meanwhile, an investigation of the physicochemical and pharmacokinetic parameters of the compounds showed that they have acceptable physicochemical and pharmacokinetic properties. However, these properties can be guided for optimization by structural modifications using a structure-based drug design approach.

As a result, our findings displayed that fruticul-A and demethylfruticul-A have the capability to be developed as excellent natural product derived CDK-2 inhibitors, and further biological experiments should be performed to confirm their use as efficient options for treating cancer.

Acknowledgments

None.

Author contributions

Hossein Hadavand Mirzaei was contributed in conceptualization, data collection and analysis, writing and editing of the manuscript; Seyed Mohammad Hosseini was involved in data collection and approving the final draft of the manuscript.

Declaration of interest

The authors declare that there is no conflict of interest. The authors alone are responsible for the accuracy and integrity of the paper content.

References

[1] Slamon D, Pegram M. Rationale for

trastuzumab (Herceptin) in adjuvant breast cancer trials. *Semin Oncol.* 2001; 28(3): 13–19.

- [2] Alam P, Tyagi R, Farah MA, Rehman MT, Hussain A, AlAjmi MF, Siddiqui NA, Al-Anazi KM, Amin S, Mujeeb M. Cytotoxicity and molecular docking analysis of racemolactone I, a new sesquiterpene lactone isolated from *Inula racemosa*. *Pharm Biol.* 2021; 59(1): 941–952.
- [3] Kolšek K, Mavri J, Sollner Dolenc M, Gobec S, Turk S. Endocrine disruptome an open source prediction tool for assessing endocrine disruption potential through nuclear receptor binding. *J Chem Inf Model.* 2014; 54(4): 1254–1267.
- [4] Gach K, Długosz A, Janecka A. The role of oxidative stress in anticancer activity of sesquiterpene lactones. *Naunyn-Schmiedeb Arch Pharmacol.* 2015; 388(5): 477–486.
- [5] Piccinelli AC, Figueiredo de Santana Aquino D, Morato PN, Kuraoka-Oliveira AM, Strapasson RLB, Dos Santos EP, Stefanello MÉA, Oliveira RJ, Kassuya CAL. Anti-inflammatory and antihyperalgesic activities of ethanolic extract and fruticul-A from *Salvia lachnostachys* leaves in mice. *Evid Based Complement Altern Med.* 2014; Article ID 835914.
- [6] Rodríguez-Hahn L, Esquivel B, Sánchez C, Estebanes L, Cárdenas J, Soriano-García M, Toscano R, Ramamoorthy T. Abietane type diterpenoids from *Salvia fruticulosa*. A revision of the structure of fruticul-B. *Phytochemistry.* 1989; 28(2): 567–570.
- [7] Bisio A, Romussi G, Russo E, Cafaggi S, Schito AM, Repetto B, De Tommasi N. Antimicrobial activity of the ornamental species *Salvia corrugata*, a potential new crop for extractive purposes. *J Agric Food Chem.* 2008; 56(22): 10468–10472.
- [8] Valant-Vetschera KM, Roitman JN, Wollenweber E. Chemodiversity of exudate flavonoids in some members of the Lamiaceae. *Biochem Syst Ecol.* 2003; 31(11): 1279–1289.
- [9] Oliveira CS, Salvador MJ, de Carvalho JE, Barison A. Cytotoxic abietane-derivative diterpenoids of *Salvia lachnostachys*. *Phytochem Lett.* 2016; 17: 140–143.
- [10] Corso CR, Stipp MC, Radulski DR, Mariott M, da Silva LM, de Souza Ramos EA, Klassen G, Queiroz Telles JE, Oliveira CS,

- Stefanello M^ÉA, Verhoeven AJ, Oude Elferink RPJ, Acco A. Fruticuline A, a chemically-defined diterpene, exerts antineoplastic effects in vitro and in vivo by multiple mechanisms. *Sci Rep.* 2020; 10(1): 1–14.
- [11] Monticone M, Bisio A, Daga A, Giannoni P, Giaretti W, Maffei M, Pfeffer U, Romeo F, Quarto R, Romussi G. Demethyl fruticuline A (SCO-1) causes apoptosis by inducing reactive oxygen species in mitochondria. *J Cell Biochem.* 2010; 111(5): 1149–1159.
- [12] Giacomelli E, Bertrand S, Nievergelt A, Zwick V, Simoes-Pires C, Marcourt L, Rivara-Minten E, Cuendet M, Bisio A, Wolfender JL. Cancer chemopreventive diterpenes from *Salvia corrugata*. *Phytochemistry.* 2013; 96: 257–264.
- [13] Pires DE, Blundell TL, Ascher DB. pkCSM: predicting small-molecule pharmacokinetic and toxicity properties using graph-based signatures. *J Med Chem.* 2015; 58(9): 4066–4072.
- [14] Mirzaei HH, Firuzi O, Jassbi AR. Diterpenoids from roots of *Salvia lachnocalyx*; in-silico and in-vitro toxicity against human cancer cell lines. *Iran J Pharm Sci.* 2020; 19(4): 85–94.
- [15] Webb B, Sali A. Comparative protein structure modeling using MODELLER. *Curr Protoc Bioinformatics.* 2016; 54(1): 1–57.
- [16] Morris GM, Huey R, Lindstrom W, Sanner MF, Belew RK, Goodsell DS, Olson AJ. AutoDock4 and AutoDockTools4: Automated docking with selective receptor flexibility. *J Comput Chem.* 2009; 30(16): 2785–2791.
- [17] Daina A, Michielin O, Zoete V. SwissADME: a free web tool to evaluate pharmacokinetics, drug-likeness and medicinal chemistry friendliness of small molecules. *Sci Rep.* 2017; 7: 1–13.
- [18] Daina A, Zoete V. A boiled-egg to predict gastrointestinal absorption and brain penetration of small molecules. *Chem Med Chem.* 2016; 11(11): 1117–1121.
- [19] Laskowski RA, MacArthur MW, Moss DS, Thornton JM. PROCHECK: a program to check the stereochemical quality of protein structures. *J Appl Crystallogr.* 1993; 26(2): 283–291.
- [20] Kawatsuki A, Yasunaga J, Mitobe Y, Green PL, Matsuoka M. HTLV-1 bZIP factor protein targets the Rb/E2F-1 pathway to promote proliferation and apoptosis of primary CD4+ T cells. *Oncogene.* 2016; 35(34): 4509–4517.
- [21] Gurung AB, Ali MA, Lee J, Farah MA, Al-Anazi KM. Molecular docking and dynamics simulation study of bioactive compounds from *Ficus carica* L. with important anticancer drug targets. *PLoS One.* 2021; Article ID 0254035.

Abbreviations

CDK-2: cyclin-dependent protein kinase 2; CDK-6: cyclin-dependent protein kinase 6; topo I: DNA topoisomerases I; topo II: DNA topoisomerases II; Bcl-2: B-cell lymphoma-2; ns: nanosecond; HDACs: histone deacetylases family; ADT: Autodock; MD: molecular dynamic; ADMET: absorption, distribution, metabolism, excretion, and toxicity; 3D: three-dimensional structures; G09: Gaussian 09; NVT: number of particles, volume and temperature; NPT: number of particles, pressure and temperature; PME: particle mesh ewald; RMSD: root mean square deviation; RMSF: root means square fluctuation; Rg: radius of gyration